Chapter 2

Stellar Population Models I: Are the IRS 16 Stars Expected to be Hot?

Peter Tamblyn & G. H. Rieke

Abstract

We have constructed burst models of the stellar population in the Galactic center. Many classes of models can be excluded entirely. Models with an age of 7 to 8 Myr and an initial mass of less than 4×10^5 $M_\odot$ can reproduce the red supergiant stars and stars with the continuum characteristics of IRS 16 and provide the ionizing flux. We show that if IRS 16 is the product of normal stellar evolution associated with a recent star formation burst that currently dominates the energetics of the region, then IRS 16 itself is inconsequential to Galactic center energetics.

2.1 Introduction

The large amount of foreground extinction in the direction of the Galactic center (GC) has hampered investigations of the energy source for this region. However, it has become apparent that there are a number of very young stars in the area (e.g., Lebofsky, Rieke, & Tokunaga 1982) and it appears that energy is provided by more than one object (Rieke, Rieke, & Paul 1989). These observations suggest the hypothesis that a burst of recent star formation is the primary energy source. Unfortunately, infrared colors are uninformative in identifying hot stars that are candidates to supply this energy because they sample only the Rayleigh-Jeans tails of the energy distributions. In this chapter we combine the available spectral type information for the brightest sources with other observational constraints to investigate star formation burst models consistent with the observed characteristics of the GC.

IRS 16 is a collection of bright sources with relatively hot spectral energy distributions which some authors (cf. Allen, Hyland, & Hillier 1990) have suggested may be responsible for the majority of the ionizing radiation in the GC environment. The exact nature of IRS 16 is hidden by the obscuring dust; but by postulating that IRS 16 is a collection of normal stars associated with a recent burst of star formation, we can probe the characteristics of these sources indirectly.

In this study, we construct synthetic bursts with Monte-Carlo generated populations of stars, aged according to theoretical stellar evolutionary tracks. A model is judged successful if it explains the observed stars and meets the mass and ionizing radiation field constraints as described in Section 2.2. In Section 2.3 we detail the construction of the burst models. Section 2.4 uses the burst models to eliminate classes of solutions which are inconsistent with the observational constraints. Sections 2.5 and 2.6 describe the solutions we find and their implications.

2.2 Observational Constraints

2.2.1 Mass

A variety of techniques have been used to study the dynamics and mass distribution in the central 1–2 pc of the galaxy (Rieke & Rieke 1988; McGinn *et al.* 1989; Serabyn *et al.* 1988). Within a 1 pc radius, it is found that the total mass is $\sim 3.5 \times 10^6\,M_\odot$ of which $\sim 2.5 \times 10^6\,M_\odot$ is some form of centrally concentrated matter. Allowing for the mass of the old stellar population, we require that the recent burst of star formation involve a mass no greater than $4 \times 10^5\,M_\odot$.

2.2.2 Ionizing Radiation Field

The GC has a high density of UV radiation ($\gtrsim 10^{50}\,\mathrm{photon\,s^{-1}}$) with a soft ($T_{\mathrm{eff}} \lesssim 35,000\,\mathrm{K}$) spectral distribution (Lacy *et al.* 1980; Serabyn & Lacy 1985). A few stars hotter than 35,000 K could exist at the GC so long as their contribution to the total ionizing radiation field is small. We required that bursts have less than 20% of their ionizing flux from stars hotter than 37,000 K. The models are quite insensitive to the ratio selected.

2.2.3 IRS 16

IRS 16 seems to be a promising candidate for the ionizing source. Simons, Hodapp, & Becklin (1990) calculated that if IRS 16 is composed of 4 O7 supergiants with surface temperatures of order 35,000 K, it could provide all of the ionizing radiation and 20% of the total luminosity. IRS 16 has been resolved into 4 dominant components (Simon *et al.* 1990; Simons *et al.* 1990). The presence of He I emission from the gas surrounding these components lends credence to the theory that they are energetic.

IRS 16 components NE and NW have K magnitudes of 8.68 and 8.78 respectively (Rieke *et al.* 1989). Component C and the dominant source in SW are approximately

one magnitude fainter (Simons *et al.* 1990). At the distance to the GC ($\approx 8\,\mathrm{kpc}$) and with an extinction A_K of 3.47 (Rieke *et al.* 1989), these sources have absolute K magnitudes ~ -8.3 to -9.3. The high-resolution observations obtained during lunar occultations of IRS 16 by Simons *et al.* (1990) indicate that the dominant components have diameters less than $0.02''$ which corresponds to 160 AU at the distance of the GC. Hence, it is extremely improbable that these components are themselves aggregates of stars. Their near-infrared colors are consistent with Rayleigh-Jeans tails from relatively hot sources. The absence of detectable CO absorption indicates a lower limit on the temperature of the sources (e.g., Allen *et al.* 1990). The precise temperature at which CO absorption would be undetectable at high metallicity with an allowance for unknown surface gravity is difficult to pin down, but 5,000 K is an adequately generous lower limit. The UV temperature constraint applies as an upper limit to the temperature of IRS 16 because if as hot as 35,000 K, IRS 16 would produce $\sim 10^{51}$ ionizing photons per second (based on model stellar atmospheres, as described in Section 2.3.4). These temperature limits allow considerable latitude in the nature of IRS 16. If near the upper end of the allowed temperature range, IRS 16 is one of the primary energy and UV sources in the GC; if at the low end its UV output would be negligible. We can estimate the total luminosity of each of these sources as a function of their effective temperatures by assuming a blackbody energy distribution. This defines a locus in the HR diagram in which stars would appear as IRS 16 components.

2.2.4 Red Supergiant Stars

In the inner 2 parsecs of the GC field there are 9 stars with spectral classifications M0 to M4 in luminosity classes I and II (Rieke *et al.* 1989). Comparison with bulge giants (Frogel *et al.* 1978; Schmidt-Kaler 1982; Frogel & Whitford 1987) with a generous allowance for metallicity effects suggests limits on T_{eff} of 4,170 K and

2,800 K for these stars. Luminosities of the GC red supergiants (RSGs) are in the range 10^4 to 10^6 $L_\odot$.

2.3 Models of the Stellar Population

A model of a stellar population is fundamentally a sum of the characteristics of a group of stars. The age distribution of stars in the models, normalization of the models, distribution of stellar types, and evaluation of the stars' characteristics are discussed in this section.

2.3.1 Age Distribution

The hypothesis for this analysis is that most of the energetic phenomena at the GC are caused by young stars. As these stars have short lifetimes a burst is most efficient at producing the stars of interest. A spread in ages might be a more appropriate model for real star formation, but would dilute our results in this analysis.

2.3.2 Stellar Distribution

The initial mass function (IMF) describes the relative numbers of stars created in an episode of star formation as a function of their initial mass. However, the IMF is an averaged distribution. If a small number of stars are created in a single event, sample statistics can distort the mass distribution of stars compared with the predictions of a smooth IMF. Sample variations are particularly evident in the upper mass ranges: even a large burst of star formation will have only a relative handful of the most massive and most luminous stars. Yet, the observable characteristics of a population of stars are often dominated by the few most luminous members. Hence, two bursts with identical average characteristics could have very different observational characteristics due to small sample statistics. To overcome this limitation, we have used the technique of Monte-Carlo integration. By repeating a set of tests

with many different randomly populated bursts, we can estimate the probability of a burst with given parameters leading to the observed GC population.

The initial masses of the stars were distributed randomly in accordance with a power-law approximation to a Miller-Scalo (1979) IMF extended to $100\,M_\odot$ [only relevant for the youngest bursts]. A randomly generated number (x) between zero and one was mapped to an initial mass M:

$$M = ((M_u^{-\alpha+1} - M_l^{-\alpha+1})x + M_l^{-\alpha+1})^{\frac{1}{-\alpha+1}} \tag{2.1}$$

where α is the IMF power law index (3.3 for a Miller-Scalo IMF). M_u is the mass of the most massive star still in existence at the specified burst age in accordance with the linear interpolation used between source tracks. M_l is the mass of the lowest-mass stars of interest, taken to be $10\,M_\odot$ for this analysis. Stars with masses 0.1–$10\,M_\odot$ contribute relatively little ionizing flux but were considered when computing the mass and luminosity of each burst.

2.3.3 Stellar Evolutionary Tracks

Rich (1990) has found a wide spread in metallicities of nuclear bulge giants with an average metallicity of approximately twice solar. The abundances in the interstellar medium in the GC (out of which the burst stars would have formed) are difficult to determine because of reddening and other effects, but are estimated to be roughly twice solar (Lacy *et al.* 1980).

The accuracy of any analysis of this sort is fundamentally limited by the accuracy of the input stellar evolutionary tracks. The dearth of easily observable stars in the relevant mass range, and observational ambiguities including distance and interstellar reddening (Conti 1988), have led to uncertainties in the tracks. Convective overshoot and mass loss are of great importance to the evolution of massive stars, yet their extent is unclear (Schaller *et al.* 1992, hereafter SSMM). The obser-

vational evidence that the GC has a metallicity well above solar compels us to use evolutionary tracks which are less well constrained than those for solar metallicity. Non-solar metallicity introduces uncertainties in abundance ratios, opacities, and mass-loss rates (Conti 1988). However, our analysis yields a well defined conclusion that is likely to be correct qualitatively despite uncertainties in the evolutionary tracks.

We based one set of models on Maeder's (1990) stellar evolutionary tracks for massive stars with Z=0.040. These tracks have metallicity-dependent mass-loss rates and moderate convective overshoot. The tracks are tabulated by evolutionary stage such that one can interpolate between similar stages of evolution in neighboring source tracks. For each model star, a track segment for the randomly generated mass was interpolated from the set of source tracks and, at the chosen age, the luminosity, temperature, and current mass were interpolated from this segment.

For comparison we repeated our modeling with stellar evolutionary tracks published by SSMM for solar metallicity. These tracks differ from the Maeder tracks in many respects as detailed by SSMM. Of most importance for this analysis are revisions to the nuclear cross-sections which affect the blue loops, reduction of various timescales due to a change in the method used to compute compositions which is especially important in the presence of convective overshoot, and the treatment of the optically thick winds of WR stars in accordance with Castor, Abbott, & Klein (1975) theory. These differences apparently dominate the metallicity differences for most of the behaviors relevant for this paper. Tracks for $20\,M_\odot$ and up are published with standard mass-loss rates [set C] and with doubled mass-loss rates in the post-main-sequence stages [set D]. SSMM favor the latter to match observations of WR stars. Stars at the GC are likely to have enhanced mass loss due to the high ambient UV field and super-solar metallicity. The mass-loss rate has a dramatic

impact on the parameters of interest in this analysis, so complete sets of models were run with both sets of tracks.

Figure 2.1 illustrates burst models at various ages based on the three sets of stellar evolutionary tracks. Comparison reveals the very different behaviors described by the tracks in the post-main-sequence stages of evolution. In particular, the very hot and luminous Wolf-Rayet stars at the left of the 6 and 7 Myr panels of the Maeder bursts are much less numerous (because of reduced timescales) in bursts based on the SSMM tracks. The fraction of stars in blue loop phases of evolution is greatly reduced in the models based on the SSMM tracks.

2.3.4 Ionizing Radiation

Each burst model was constructed by adding stars to the burst until the ionizing flux from the collection of aged stars was $\geq 10^{50}\,\mathrm{photon\,s^{-1}}$. The Lyman contributions of model atmospheres were integrated from Kurucz (1992) synthetic stellar spectra for Z=0.04. The optically thick winds of Wolf-Rayet stars have strongly wavelength dependent optical depth effects which distort the emergent spectrum dramatically. The Kurucz atmospheres are assumed LTE and planar, neither of which applies to these winds. Care must be taken to consider the large uncertainties when interpreting burst models in which these stars are prominent.

Maeder (1990) only has tracks for stellar masses $15\,M_\odot$ and greater. At early ages the relative contribution to the UV flux from lower-mass stars is negligible. However, as the burst ages, the fractional contribution of the lower-mass stars grows and dominates the UV flux at ages greater than about 8 Myr. To make models of bursts at these ages, it was necessary to estimate the UV contribution from stars less massive than the Maeder tracks described. From our results, bursts older than 8.5 Myr cannot fit the characteristics of the GC. By restricting our analyses to ages less than 9.6 Myr, we were able to ensure that all stars in the burst less massive than

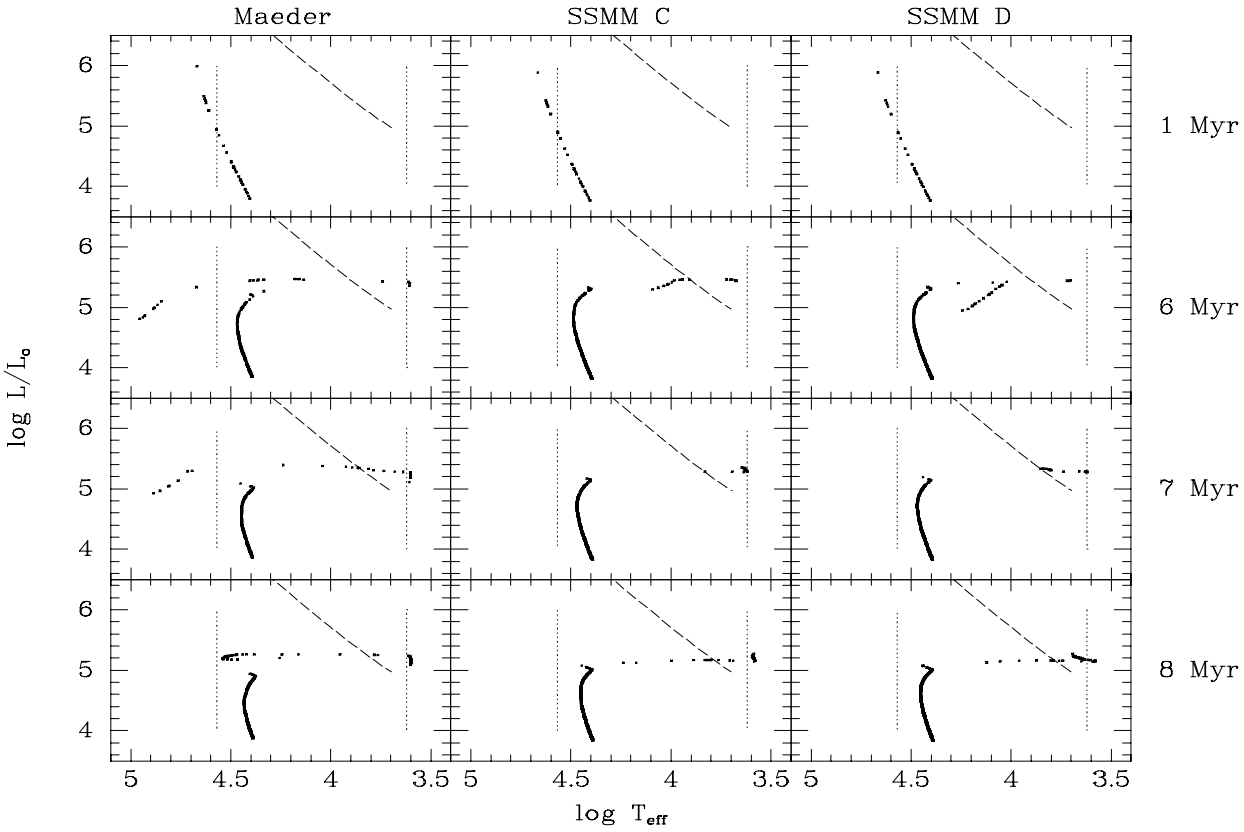

Figure 2.1: Synthetic Burst HR Diagrams at Various Ages. Dotted lines at $T_{\rm eff} = 37,000\,{\rm K}$ and at 4,170 K represent the cutoffs used for the UV temperature constraint and RSG counts. The dashed line is the locus of blackbodies with $M_K = -9.3$ (IRS 16-like sources). Note that many more stars are needed at later ages to produce the same Lyman flux and that candidate IRS 16 stars are progressively cooler in older bursts. It is also apparent that young bursts do not have the red stars observed at the GC. The differences in post-main-sequence evolutionary behaviors of the sets of tracks are quite apparent.

15 $M_\odot$ were still on the Main Sequence. A comparison of evolutionary tracks for 15 $M_\odot$ reveals that main-sequence evolution of SSMM tracks for Z=0.02 is similar to the evolution described by the Maeder tracks. An overall increase in luminosity of 8% and a decrease in main-sequence lifetime of 8% applied to the SSMM track made the main-sequence portions of the 15 $M_\odot$ tracks from these two sources essentially identical. To supplement the Maeder tracks, these same corrections were applied to the 12 and 9 $M_\odot$ tracks from SSMM and tracks interpolated in the 10 to 15 $M_\odot$ range in the same manner as with the Maeder tracks. Contributions from these stars were always tallied separately to make it apparent when errors in this procedure might influence results.

2.3.5 Burst Tests

Once the normalized burst population had been synthesized, a series of quantitative tests were applied to determine if the model burst matched the observed GC. The first of these tests was to check that the total ionizing photon fluxes from stars with $T_{\rm eff} < 37,000$ K was at least four times as great as the ionizing fluxes from hotter stars. The second test is that the total initial mass of the burst be less than 4×10^5 $M_\odot$. The number of stars in a burst model was determined by adding massive stars until the aggregate produced adequate UV output. The total mass of stars was determined by integrating the normalized Miller-Scalo (1979) IMF extended to 100 $M_\odot$:

$$M_{total} = \frac{N}{\int_{10}^{M_u} \psi(m) dm} \times \int_{0.1}^{100} \psi(m) m dm \qquad (2.2)$$

in which m has units of solar masses, N is the number of massive stars in a burst, and M_u is the same as in Equation 2.1.

Finally, the model burst must reproduce the observed stellar population. Model stars with blackbody-approximated M_K in the range -8.81 to -9.69 (0.67 to 1.5 times the luminosity of a bright IRS 16 component at the same temperature) were

tallied as IRS 16-like sources; four had to be in a synthetic burst for it to be considered a successful GC match. Model stars which get as cool as $T_{\rm eff}$=4,170 K have luminosities in the range observed for RSGs at the GC. A count of all stars in this temperature range was kept and required to be between 7 and 15 for a successful GC model. The star count restrictions are generous to compensate for the instantaneous star formation history we assumed for bursts. For example, although a burst model with a particular age might make more IRS 16-like stars than are observed, only a small spread in ages around this value would result in significantly reduced IRS 16 counts.

Table 2.1 lists the tests a burst model was required to pass to be counted as a successful model of the GC. Figure 2.2 summarizes the behavior of models using the Maeder Z=0.04 tracks. Figures 2.2*a*-*e* plot the average values of the portion of ionizing radiation from stars with $T_{\rm eff}$ above 37,000 K, the ratio and numbers of RSG and IRS 16 stars, and the total initial mass of stars. Figure 2.2*f* plots the percentage of bursts which satisfied these criteria as a function of age — in this case none. The models based on the Maeder Z=0.04 tracks fail primarily because of the UV $T_{\rm eff}$ constraint. As mentioned above, the $T_{\rm eff}$ of the WR stars which dominate the ionizing flux at the relevant ages is uncertain, so Figure 2.3 shows the same quantities without this test applied. Figures 2.4 and 2.5 show the same quantities for the full set of tests for bursts using the SSMM stellar evolutionary tracks. The UV $T_{\rm eff}$ criterion is a redundant constraint for these models.

The bolometric luminosities associated with a starburst population (including the late-type component) sufficient to produce the ionization were calculated to be $\sim 1 \times 10^7\,{\rm L}_\odot$ at 5 Myr and $\sim 8 \times 10^7\,{\rm L}_\odot$ at 8 Myr. These values are generally toward the high end of the estimated range (Werner & Davidson 1989) but they are compatible with observation if the solid angle subtended at the luminous stars by

Table 2.1: Criteria for Galactic Center-like Bursts

UV flux	$\geq 10^{50} \gamma\, \mathrm{s}^{-1}$
UV T_{eff}	Ionizing photon flux from stars with
	$T_{\mathrm{eff}} > 37,000\, K$ required to be $< 20\%$ of total
Initial mass	$\leq 4 \times 10^5\, \mathrm{M}_\odot$
# RSG	7 to 15
# IRS 16	≥ 4

the dust torus is as small as indicated by the observations of Güsten *et al.* (1987).

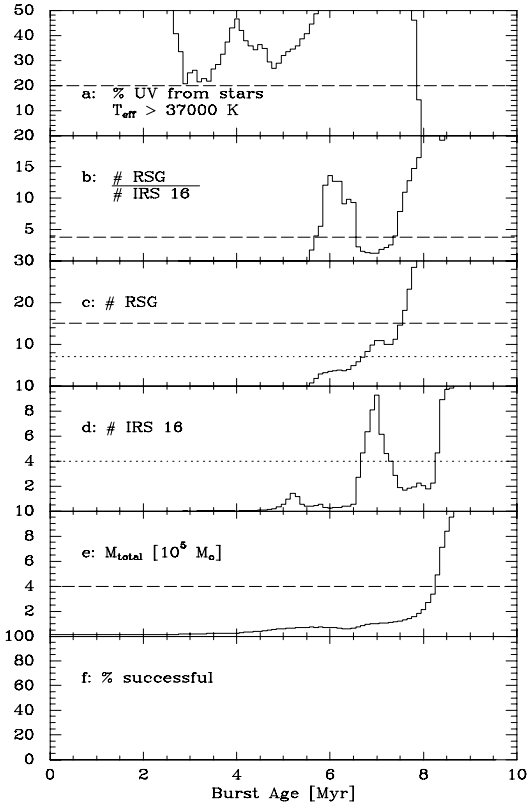

Figure 2.2: Average Quantities from 500 Synthetic Bursts Based on the Maeder Z=0.04 Stellar Evolutionary Tracks. Upper and lower limits are represented by dashed and dotted lines respectively. Panel *a* is the portion of the summed ionizing photon fluxes from stars hotter than 37,000 K; *b* is the ratio of RSGs to IRS 16-like sources; *c* is the number of RSGs; *d* is the number of IRS 16-like sources; *e* is the mass formed into stars in units of $10^5\,M_\odot$; *f* is the percentage of models that met all constraints.

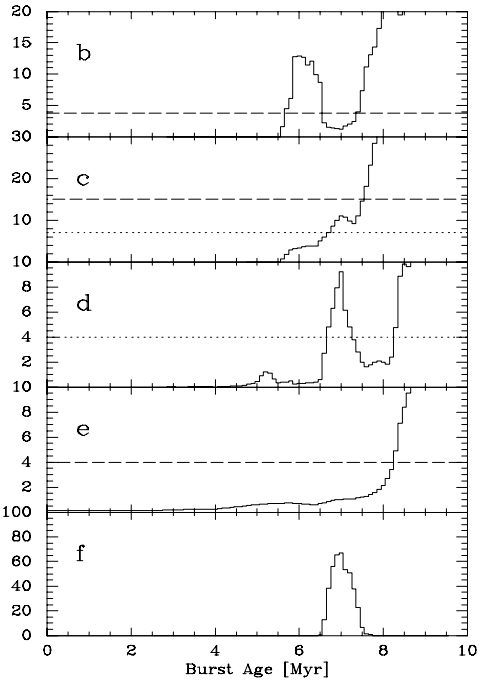

Figure 2.3: Same as Figure 2.2 with the UV $T_{\rm eff}$ constraint suppressed.

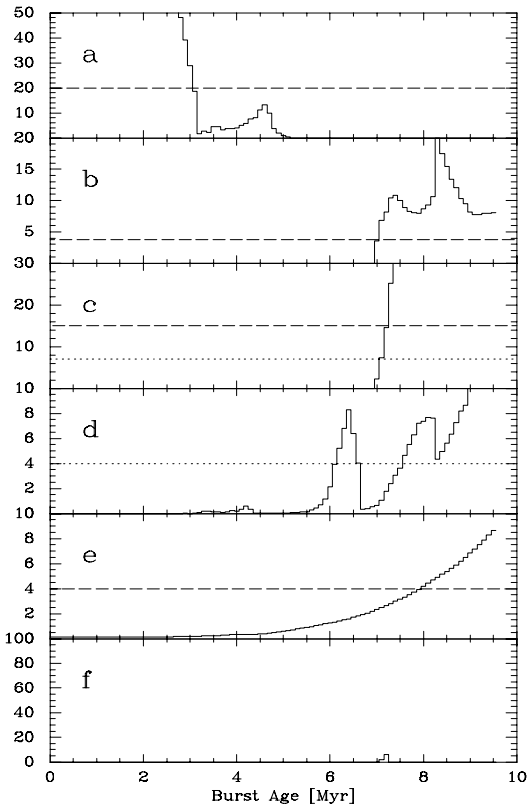

Figure 2.4: Same as Figure 2.2 with SSMM stellar evolutionary tracks with standard post-main-sequence mass-loss rates.

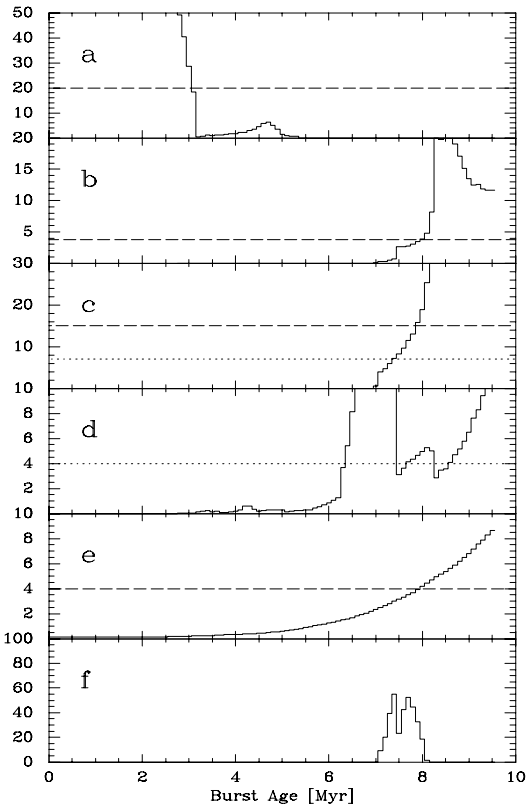

Figure 2.5: Same as Figure 2.2 with SSMM stellar evolutionary tracks with doubled post-main-sequence mass-loss rates.

2.4 Excluded Ages

2.4.1 Simple Star Formation History

Examination of Figures 2.2–2.5 allows us to exclude with confidence various ages of bursts. The youngest bursts are excluded by the constraint on the UV spectrum and because they do not produce any RSGs nor sources which would have IRS 16's observed characteristics. All three tests are independent of normalization and of each other. There continue to be no stars as cool as the GC RSGs until 5.5 Myr with the Maeder tracks and until 6.9 Myr with the SSMM tracks.

Bursts older than 8.5 Myr can also be dismissed. If stars are responsible for all of the Lyman photons, then these bursts require that more mass was converted into stars in the star formation episode than the dynamical observations allow and too many RSGs are present. Further, these bursts overproduce RSG stars relative to stars in the IRS 16 locus. Additional sets of models were computed with the SSMM tracks to confirm that this ratio remains well above the upper limit at ages later than shown in Figures 2.4 and 2.5. Note that this ratio is independent of normalization.

Although the mass, UV $T_{\rm eff}$, and IRS 16 count constraints confirm the result, the RSG count is sufficient to limit the ages of consistent bursts to a very narrow range (assuming that young stars provide the ionizing radiation). Even without this normalization assumption the models indicate that ages outside the range 5.5–8 Myr would not be likely to produce the stars observed at the GC. Therefore, our conclusions are unlikely to be affected by modifications in the IMF which might relax the mass constraint by reducing the proportion of low ($\sim$ solar) mass stars.

2.4.2 Complex Star Formation History

A more complex star formation history than just a single instantaneous burst could produce a different mix of stars observed at the present time. However, the uncer-

tainties in late stages of massive stellar evolution as illustrated by these three sets of stellar evolutionary tracks make it clear that any attempt to disentangle star formation history effects from stellar evolutionary effects would be mired in uncertainty. However, our basic conclusions do not seem to depend strongly on details of the star formation history. For example, consider models based on the tracks from set C of SSMM, which indicate the probability of a single burst reproducing the observed stellar population is very low. A mix of stars with ages 6.4 Myr, when IRS 16-like sources are relatively common, and 8.3 Myr, when RSGs are quite common, might be able to match the observed stellar population and slip in under the mass constraint. However, any such complex star formation history must still be dominated by star formation between $\sim$ 3 and 8 Myr ago to avoid having too much hard UV or mass.

2.5 Successful Models

2.5.1 Burst Parameters

The set of SSMM tracks with enhanced mass loss are the only set that yield formal solutions with high probability. The successful burst models have an age of 7–8 Myr, an initial mass of stars of a few times $10^5\,M_\odot$, and 1000–1900 stars more massive than $10\,M_\odot$ at the time of observation. Assuming $A_V = 30$ and a distance of 8 kpc, these stars have average integrated $m_K \sim 4.5$, 3.9, and 3.3 at 7.0, 7.5, and 8.0 Myr respectively, in agreement with the $m_K \sim 3.3$ within the central $1.8'$ (~ 2 pc radius) measured by Becklin & Neugebauer (1968). In successful models, the IRS 16 components are F or G supergiants with $L \sim 10^5\,L_\odot$ and $T_{\rm eff} \sim 6,000$ K. The ionization is provided by many late O or early B main-sequence stars with $T_{\rm eff} \sim 30,000$ K. The Maeder Z=0.04 tracks match all of the constraints at $\sim$ 7 Myr except the UV $T_{\rm eff}$ constraint. The WR stars left of the 37,000 K line in the relevant subpanel of

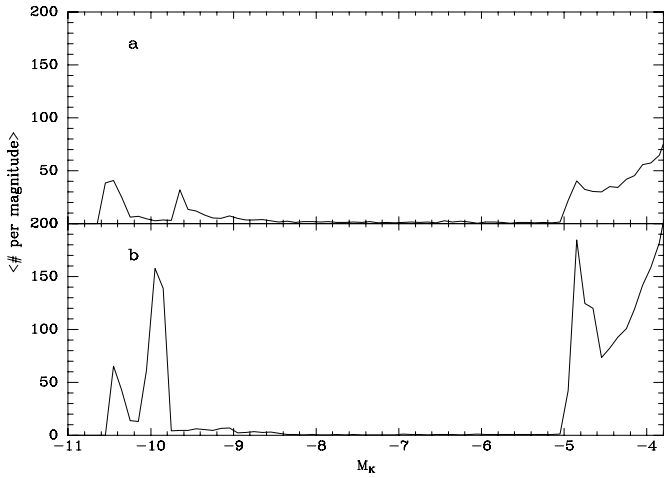

Figure 2.6: Averages of 100 Luminosity Functions. Panel *a*: models based on Maeder tracks at an age 7.0 Myr; *b*: models based on SSMM tracks at an age 7.7 Myr.

Figure 2.1 contribute only ∼7% of the luminosity but most of the ionizing photons at these ages. As discussed above, the Lyman flux and characteristic temperature of WR stars are quite uncertain so it is not necessarily the case that the $T_{\rm eff}$ is correctly represented by the tracks. The SSMM tracks with the lower mass-loss rate give very low probabilities of burst solutions because model stars do not get as cool as the GC RSGs until after the first peak in the count of IRS 16-like sources.

Predicted luminosity functions for average bursts are given in Figure 2.6 based on the Maeder tracks at age 7.0 Myr and the enhanced mass loss SSMM tracks for an age of 7.7 Myr where the probability of a GC-like burst peaks. We conclude that the currently observed very high luminosity stars are likely to be the only ones observable, even with increased sensitivity and angular resolution, since the next most luminous stars are more than 4 magnitudes fainter and will tend to be heavily confused with the old stellar population.

2.5.2 Explosive Event

There exists a body of evidence pointing to a recent powerful explosion at the GC. Townes (1989) discusses the turbulent clouds near the GC and the evacuation of the GC region as possibly indicating an explosion in the region 10^5 yr ago. Mezger *et al.* (1989) detected a dust ring with radius ~ 5 pc around the synchrotron shell source Sgr A East. The source geometry suggests that an explosion inside a giant molecular cloud broke through the near side of the cloud and created a shell structure similar to a supernova (SN) remnant. Mezger *et al.* (1989) suggest this structure is due to a powerful event at the location of Sgr A* or to a SN inside a wind blown bubble. A difficulty with the latter explanation is that the formation of a wind blown bubble of this size requires $\sim 10^6$ yr without significant tidal disruption. Nonetheless, based on the radio brightness, Mezger *et al.* (1989) conclude that such a SN would have occurred 7,500 years ago. Our models predict one SN approximately every 70,000 yr and also have stars capable of creating substantial wind bubbles. Given the uncertainties in the estimate of the timescales involved, we consider it plausible that the Sgr A East structure is a SNR associated with the burst of star formation considered in this paper.

2.6 Conclusion

We can distinguish three different hypotheses for the activity in the GC:

2.6.1 Excitation by a Burst of Star Formation, with Normal Stellar Evolution

The primary conclusion of this paper is that, should all the activity in the GC be powered by a burst of star formation after which the stars evolved normally, then the bright (in the near infrared) blue stars that lie in IRS 16 are unlikely to be the objects that actually provide the UV flux and luminosity of the region. The time

since the episode of star formation must be roughly 7 Myr, the only epoch at which the observed numbers of UV photons and blue and red stars appear simultaneously. Given this age, however, a mix of objects that reproduces the observations within the current uncertainties in theoretical stellar evolution has a significant probability of forming.

2.6.2 Excitation by Non-Stellar Means, Recent Star Formation and Normal Evolution

The UV in the GC may be provided by some non-stellar source, with the observed population of stars arising as an incidental event. In this case, we find that the relative numbers of red giants and supergiants and IRS 16-like sources never reproduces the observations except during the same interval when the stars can provide the UV. Bursts of star formation that are more than 8 Myr old produce a larger ratio of red supergiants to IRS 16-like objects than is observed, and bursts less than 5.5 Myr old do not produce enough red supergiants. A separate UV source is therefore unnecessary if normal stellar evolution occurs; a burst of star formation that accounts for the components of IRS 16 and the red supergiants has no difficulty in producing adequate UV.

2.6.3 Abnormal Stellar Evolution

The presence of IRS 7 in the GC demonstrates that massive stars have formed in this region in the last ~ 10 Myr. However, conditions in the GC may lead to stellar evolution that is significantly different from that observed elsewhere and represented by the evolutionary tracks used in our analysis. If the components of IRS 16 are hot enough to excite He I directly, for example, then we would conclude that the stellar evolution is highly abnormal or that these objects are not stars.

This work suggests a critical test for the hypothesis that a burst of star formation

with normal stellar evolution accounts for the energetics of the GC. The members of IRS 16 should not be hot enough to produce the emission of He I that is observed in close proximity to them; this gas must be ionized by hotter stars that are nearby. Applying this test may be difficult, since the unique conditions in the GC may result in excitation of He I in winds from relatively cool stars. For example, the He I imaging by Krabbe *et al.* (1991) shows strong He I from IRS 11, 12, 15E, and 17, all of which show CO bands in absorption and therefore must be dominated by red giants or supergiants. Very high resolution, spectrally resolved imaging should be used to see if the He I can be resolved separately from the continuum sources.